NUCLEAR THEORY, Vol. 37 (2018)
eds. M. Gaidarov, N. Minkov, Heron Press, Sofia

Microscopic Optical Potential Model for Analysis of the ^{12,14}Be + ^{12}C Experimental Data

E.V. Zemlyanaya[1], **V.K. Lukyanov**[1], **K.V. Lukyanov**[1], **D.N. Kadrev**[2], **M.K. Gaidarov**[2], **A.N. Antonov**[2], **K. Spasova**[2]

[1]Joint Institute for Nuclear Research, 141980 Dubna, Russia
[2]Institute for Nuclear Research and Nuclear Energy, Bulgarian Academy of Sciences, Sofia 1784, Bulgaria

Abstract. The microscopic model of optical potential (OP) is applied for calculations of the ^{12,14}Be+^{12}C elastic scattering cross sections at energies 679 MeV and 796 MeV. The real part of the OP is constructed within the double folding model with the exchange part including while the imaginary part is based on the high-energy approximation theory. The OP depends on the nuclear density distributions of ^{12,14}Be and thus, their models are tested in our study. The differential cross sections are calculated with the help of the computer code DWUCK4, in which the effect of the inelastic channel contribution is taken into account. The breakup reaction ^{14}Be+^{12}C $\rightarrow$ ^{12}Be+2n+^{12}C is also discussed.

1 Introduction

The intention of this contribution is to analyze the elastic scattering of the neutron-rich isotopes ^{12,14}Be on ^{12}C target at energy of 56 MeV per nucleon within the microscopic optical potential by using the density distribution models of the exotic nuclei ^{12,14}Be being of the main physical interest. The respective experimental data have been published in [1] and already interpreted on the basis of phenomenological approach [1, 2]. However, a reasonable agreement with the data was obtained by fitting more than 10 phenomenological parameters. Moreover, the values of parameters in [1, 2] occured to be very different from one to another. Thus, the problem is still open to explain the experimental data on the basis of a realistic theoretical approach.

In our study, the hybrid microscopic OP is used [3, 4], where the real part of the OP is constructed within the double folding model (DF) [5] with accounting for the antisymmetrization of the wave function. As to the imaginary part of the OP, it is calculated on the basis of the high energy approximation [6]. Previously, effectiveness of this approach was confirmed by analysis of experimental data on elastic cross sections and breakup of light exotic nuclei of ^{6,8}He [7–10], ^{8}B [11], ^{11}Li [12, 13], ^{10,11}Be [14].

In Section 2, the theoretical approach on the basis of the microscopic model of OP is described. The results from the analysis of the experimental data of ^{12,14}Be+^{12}C scattering are presented in Section 3. In Section 4, the approximate

theoretical estimation of the breakup cross sections of the reaction ^{14}Be+^{12}C $\rightarrow$^{12}Be+2n+^{12}C has been made.

2 Theoretical Framework

2.1 The double folding OP

The double folding OP consists of direct and exchange terms, V^D and V^{EX} [3–5]:

$$V^{DF}(r) = V^D(r) + V^{EX}(r). \tag{1}$$

Both potentials are composed from the isoscalar and isovector terms and the isoscalar one is determined by the following expressions for V^D and V^{EX}:

$$V^D(r) = \int d^3r_p d^3r_t \rho_p(\mathbf{r}_p)\rho_t(\mathbf{r}_t) v^D_{NN}(s) \tag{2}$$

$$V^{EX}(r) = \int d^3r_p d^3r_t \rho_p(\mathbf{r}_p, \mathbf{r}_p + \mathbf{s})\rho_t(\mathbf{r}_t, \mathbf{r}_t - \mathbf{s}) \times v^{EX}_{NN}(s) \exp\left[\frac{i\mathbf{K}(r)\cdot s}{M}\right]. \tag{3}$$

Here $\mathbf{s} = \mathbf{r} + \mathbf{r}_t - \mathbf{r}_p$ is the vector between two nucleons, one of which belongs to the projectile and another one to the target nucleus. $\rho_{p,t}$ are the projectile and target densities, $\mathbf{K}(r)$ is the local momentum of the nucleus-nucleus relative motion, and $v^{D,EX}_{NN}$ are the effective Paris nucleon-nucleon (NN) CDM3Y potentials parameterized in [15].

The isovector potential is determined by the same formulas (2) and (3) but ρ_i ($i = t, p$) should be exchanged by $\delta\rho_i$, the difference between proton and neutron densities for each i-nucleus.

2.2 OP within the high-energy approximation

At comparably high energies, the NN potential is expressed through its explicit form [6] and thus, the microscopical OP is presented as follows [3]:

$$U^H_{opt}(r) = -\frac{E}{k}\bar{\sigma}_N(i + \bar{\alpha}_N)\frac{1}{(2\pi)^3}\int e^{-i\mathbf{qr}}\rho_p(q)\rho_t(q)f_N(q)d^3q. \tag{4}$$

Here $\bar{\sigma}_N$ is the isospin averaged NN total cross section, $\bar{\alpha}_N$ is the ratio of real to imaginary part of the forward nucleon-nucleon amplitude, and $f_N(q) = \exp(-\beta_N q^2/2)$ where β is the slop parameter. These parameters depend on the energy and parametrized as done in [16].

So, for the imaginary potential, we obtain:

$$W^H(r) = -\frac{1}{2\pi^2}\frac{E}{k}\bar{\sigma}_N\int_0^\infty j_0(qr)\rho_p(q)\rho_t(q)f_N(q)q^2dq. \tag{5}$$

2.3 Calculation of the cross sections

The final hybrid form of the hybrid microscopic OP is following:

$$U(r) = N_R V^{DF}(r) + iN_I W^H(r), \tag{6}$$

where N_R and N_I are the renormalization factors of the real and imaginary OPs which are adjusted to experimental data, and in the case of the known densities of interacting nuclei, there are no more parameters to be fitted. The standard DWUCK4 [17] code is used for calculation of the cross sections. The Coulomb potential is taken in the standard form of the uniformly charged sphere with radius R_C.

2.4 Density distributions

In our analysis, we use the following densities of ^{12,14}Be:

- Microscopic density calculated within the generator coordinate method (GCM) [18]. In this framework, the ^{14}Be nucleus is considered as a three-cluster nucleus, involving several ^{12}Be+n+n configurations. The ^{12}Be core nucleus is described in the harmonic oscillator model with all possible configurations in the p shell.
- In the variational Monte Carlo model (VMC) [19], the proton and neutron densities are computed with the AV18+UX Hamiltonian, in which the Argonne v18 two-nucleon and Urbana X three-nucleon potentials are used.
- Phenomenological density in the form of the symmetrized Fermi function (SF):

$$\rho_{SF}(r) = \rho_0 \frac{\sinh(\frac{R}{a})}{\cosh(\frac{r}{a}) + \cosh(\frac{R}{a})},\ \rho_0 = \frac{A}{\frac{4}{3}\pi R^3}\left[1 + (\pi\frac{a}{R})^2)\right]^{-1}. \tag{7}$$

  The parameters, radius R and diffuseness a in the SF-function (7), were established in [20] by fitting (within the Glauber approach) to the experimental data of the ^{12,14}Be+p elastic scattering at 700 MeV: $R = 1.37$ fm, $a = 0.67$ fm in the case of the ^{12}Be nucleus and $R = 0.99$ fm, $a = 0.84$ fm for ^{14}Be.

Figure 1 shows the densities of ^{12}Be (left panel) and ^{14}B (central panel) that we use further in the calculations of cross sections. The solid lines correspond the GCM density, dashed lines show the SF densities, and the VMC density of ^{12}Be is shown by the dotted line.

The ^{12}C density is taken in the SF form (7) with radius 2.275 fm and diffuseness 0.393 fm. Additionally, the modified SF density was also used in our calculations:

$$\rho(r) = \rho_{SF}(r) + \rho^{(1)}_{SF}(r), \tag{8}$$

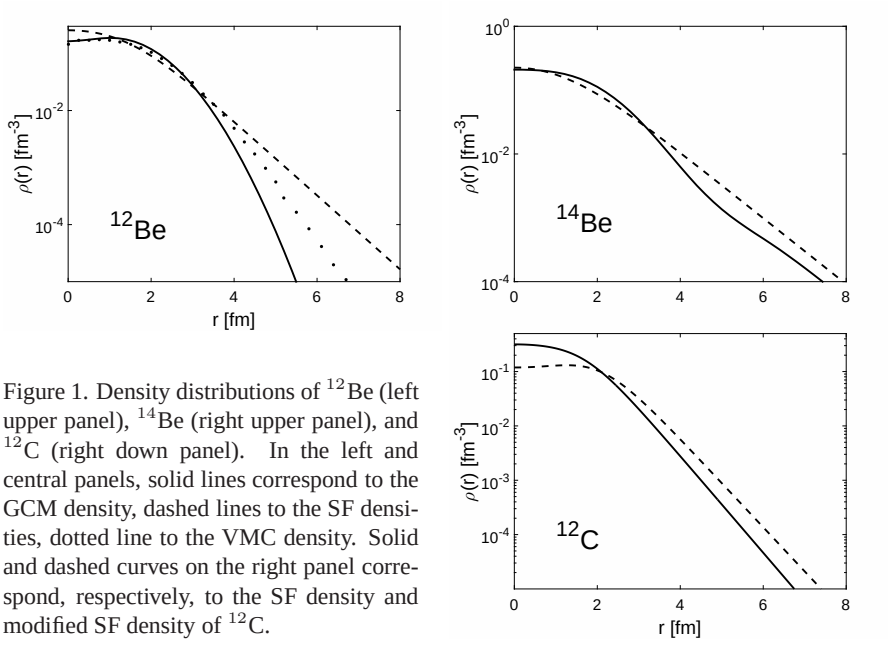

Figure 1. Density distributions of ^{12}Be (left upper panel), ^{14}Be (right upper panel), and ^{12}C (right down panel). In the left and central panels, solid lines correspond to the GCM density, dashed lines to the SF densities, dotted line to the VMC density. Solid and dashed curves on the right panel correspond, respectively, to the SF density and modified SF density of ^{12}C.

where the surface term $\rho^{(1)}$ is calculated via the 1st derivative of ρ_{SF}. Parameters of this density were obtained in [21] by fitting to eA scattering data. The ^{12}C densities are shown on the right panel of Figure 1, where the SF density is plotted by solid line and the modified density (8) by dashed line.

3 Results

The differential cross sections of the ^{12,14}Be+^{12}C elastic scattering are presented in Figure 2. Here, the standard SF form (7) of the ^{12}C density was used (R =2.275 fm and a =0.393 fm). The solid, dashed and dotted lines correspond, respectively, to the GCM, SF, and VMC densities of ^{12,14}Be. The respective values of parameters N_R and N_I are given in the Table 1. It is seen that all density models of ^{12,14}Be can not provide a reliable agreement with experimental data, especially in the small angles region: the first minimum of the calculated curves is so deep and shifted to the right in comparison to the experimental data.

Figure 3 presents the calculation with the modified SF density of ^{12}C in the form (8) in comparison with calculation using the "standard" SF density (7). The values of the parameters N_R and N_I are given in Table 1. It is seen that the modification (8) provides the left-shift correction of the first minimum of the theoretical curve. However, the agreement with experimental data stays not too good. Here the calculation with the GCM form of the ^{12,14}Be density is shown. The results for another densities are the same.

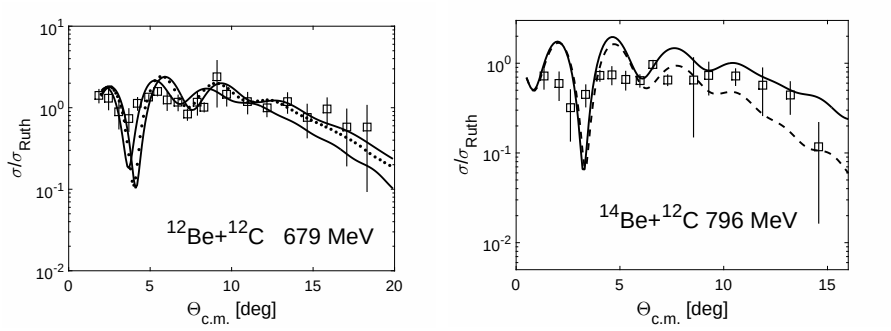

Figure 2. The differential cross sections of the ^{12,14}Be+^{12}C elastic scattering. The solid, dashed and dotted lines correspond, respectively, to the GCM, SF, and VMC densities of ^{12,14}Be.

Table 1. Values of parameters of microscopic OP

Nucleus	Density	Figure 2		Figure 3		Figure 4		
		N_R	N_I	N_R	N_I	N_R	N_I	β_{2+}
^{12}Be	GCM	0.71	0.58	0.71	0.58	0.42	1.09	0.66
	SF	0.61	0.66			0.57	0.91	0.78
	VMC	0.64	0.71			0.42	1.10	0.59
^{14}Be	GCM	0.75	1.05	0.75	1.05	0.36	1.32	0.42
	SF	0.57	0.57			0.43	0.62	0.48

At the next stage of our study we followed the notifications in [1] and [2], where the authors suggested that the experimental data should be considered as quasielastic scattering, $i.e.$, a contribution of the inelastic channels connected with excitations of the low-lying collective states of a nucleus, should be ac-

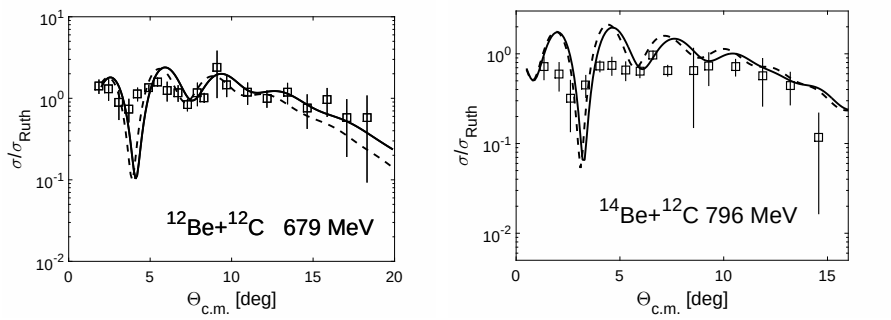

Figure 3. The differential cross sections of the ^{12,14}Be+^{12}C elastic scattering with the GCM density of ^{12,14}Be. The solid and dashed curves correspond, respectively, to the calculation with the "standard" and modified SF density of ^{12}C.

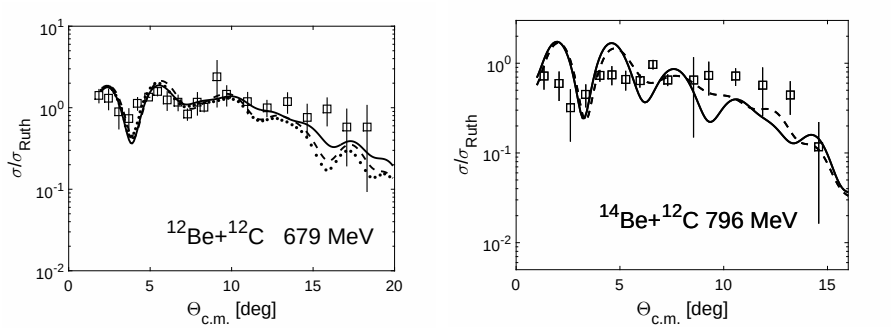

Figure 4. The differential cross sections of the ^{12,14}Be+^{12}C quasielastic scattering with accounting for the 2^+ channel. The solid, dashed, and dotted lines correspond, respectively, to the GCM, SF, and VMC densities of ^{12,14}Be.

counted for, too. Within our microscopic approach the inelastic OP was calculated via the derivative of the microscopic OPs: $U_{inel} = -\tilde{R}\cdot dU/dr$ where U is microscopic OP in the form (6), $\tilde{R}$ is the potential radius (we put $\tilde{R} = 4.25$ fm, as in [1]). As a first step, we only accounted for excitation of the 2^+ state ($E_{2+} = 4.436$ MeV). In this case, there is one more fitting parameter, namely the deformation parameter β_{2+}. The results are shown in Figure 4. The calculations have been performed with modified SF density of ^{12}C and different densities of ^{12,14}Be. The values of the parameters N_R, N_I, and β_{2+} are given in Table 1.

It is seen that the account for the inelastic channel significantly improves the agreement with experimental data although a discrepancies with experimental data are noticeable yet in the case of ^{14}Be. One expects that accounting for excitation of the 3^- inelastic channel can provide the agreement with experimental data to be comparable with results in [1, 2] on the basis of phenomenological approach.

4 Estimation of the Breakup Cross Section

The cross section of ^{14}Be+^{12}C $\to$^{12}Be+2n+^{12}C for the s-state of relative motion of the clusters ^{12}Be and $2n$ is

$$\frac{d\sigma}{dk} \sim \frac{1}{k^2}\left|\int dr\, u_{k,0}(r) g_0(r) \int d^2b\, d\cos\theta\, d\varphi\, S_c(\mathbf{b}_c) S_v(\mathbf{b}_v)\right|^2. \qquad (9)$$

Here $g_0(r)$ and $u_{k,0}$ are the bound (before) and non-bound (after breakup) cluster wave functions of ^{12}Be+$2n$. When neglecting interactions of the clusters with the target nucleus ^{12}C one gets the respective S-matrix $S_c(\mathbf{b}_c) = S_v(\mathbf{b}_v) = 1$, and thus

$$\frac{d\sigma}{dk} \sim \frac{1}{k^2}\left|\int dr\, u_{k,0}(r)\, g_0(r)\right|^2 \qquad (10)$$

Substituting here the free motion wave function $u_{k,0}$ and the oscillator wave function g_0 with binding energy E_b =1.31 MeV in the nucleus ^{14}Be=^{12}Be+2n

$$u_{k,0}(r) \,=\, \sin kr, \qquad g_0(r) \,=\, C\, r\, \exp(-\kappa r^2), \qquad \kappa \,=\, \frac{\mu E_b}{3\hbar^2} \tag{11}$$

one obtains

$$\frac{d\sigma_{\rm diff}}{dk} \,\sim\, \frac{1}{k^2}\left|\int dr\, r\, e^{-\kappa r^2}\, \sin kr\right|^2 \,\sim\, \exp\left(-\frac{k^2}{2\kappa}\right). \tag{12}$$

Substituting here κ=0.018 fm^{-2} and measuring k in units MeV/c, one gets

$$\frac{d\sigma}{dk} \,\sim\, \exp\left(-0.00072\, k^2\right). \tag{13}$$

Using Eq. (13) one obtains the widths of the momentum distribution Γ from the ratio $0.00072 \cdot (\Gamma/2)^2 \,=\, \ln 2$, which leads to the estimation $\Gamma \,=\, 62$ MeV/c comparable with the experimental value that is about 87 MeV/c [1]. One sees that we need an account for (*a*) the distortion effects when $S_c S_v$ is not equal 1, then (*b*) one should use the exact numerical wave function $u_l(r)$, and also to include contributions of the other l, L waves non equal to zero.

5 Summary

- The differential cross sections of elastic scattering of ^{12,14}Be+^{12}C at energy 56 MeV/nucleon have been analyzed within the hybrid model of microscopic optical potential.
- Three models of the ^{12,14}Be density distribution are tested.
- It was shown that the inelastic channel should be added to the elastic one to explain the experimental data of the ^{12,14}Be+^{12}C elastic scattering with given resolution.
- The approximate estimation of the width of the ^{14}Be breakup momentum distribution has been obtained to be comparable with the experimental value.

Acknowledgements

This work is partly supported by the grant of the "JINR-Bulgaria" Program, by the DFNI-T02/19 and DNTS/Russia 01/3 grants of the Bulgarian Science Foundation and by the Russian Foundation for Basic Research (grand No. 17-52-18057-bolg-A). This financial support is gratefully acknowledged.

References

[1] M. Zahar *et al.* (1994) *Phys. Rev. C* **49** 1540–1544.

[2] M.C. Mermaz (1994) *Phys. Rev. C* **50** 2620–2623.

[3] V.K. Lukyanov, E.V. Zemlyanaya, and K.V. Lukyanov (2006) *Phys. At. Nucl.* **69** 240–254.

[4] K.V. Lukyanov (2007) *JINR Communication* **R11-2007-38** Dubna.

[5] D.T. Khoa and G.R. Satchler (2000) *Nucl. Phys. A* **668** 3–41.

[6] R.J. Glauber (1959) *Lectures in Theoretical Physics*, New York: Interscience 315.

[7] V.K. Lukyanov, E.V. Zemlyanaya, S.E. Massen, Ch.C. Moustakidis, A.N. Antonov, and G.Z. Krumova (2004) *Int. J. Mod. Phys. E* **13** 573–583.

[8] V.K. Lukyanov, K.V. Lukyanov, E.V. Zemlyanaya, A.N. Antonov, and M.K. Gaidarov (2007) *Eur. Phys. J. A* **33** 389–400.

[9] V.K. Lukyanov, E.V. Zemlyanaya, K.V. Lukyanov, D.N. Kadrev, A.N. Antonov, M.K. Gaidarov, and S.E. Massen (2009) *Phys. Rev. C* **80** 024609.

[10] V.K. Lukyanov, D.N. Kadrev, E.V. Zemlyanaya, A.N. Antonov, K.V. Lukyanov, and M.K. Gaidarov (2010) *Phys. Rev. C* **82** 024604.

[11] V.K. Lukyanov, D.N. Kadrev, E.V. Zemlyanaya, K.V. Lukyanov, A.N. Antonov, M.K. Gaidarov, and K. Spasova (2017) *Eur. Phys. J. A* **53** 31.

[12] V.K. Lukyanov, D.N. Kadrev, E.V. Zemlyanaya, A.N. Antonov, K.V. Lukyanov, M.K. Gaidarov, and K. Spasova (2013) *Phys. Rev. C* **88** 034612.

[13] V.K. Lukyanov, E.V. Zemlyanaya, and K.V. Lukyanov (2015) *Phys. At. Nucl.* **78** 142–150.

[14] V.K. Lukyanov, D.N. Kadrev, E.V. Zemlyanaya, K. Spasova, K.V. Lukyanov, A.N. Antonov, and M.K. Gaidarov (2015) *Phys. Rev. C* **91** 034606.

[15] N. Anantaraman, H. Toki, and G.F. Bertsch (1983) *Nucl. Rev. A* **398** 269–278.

[16] P. Shucla (2003) *Phys. Rev. C* **67** 054607.

[17] P.D. Kunz and E. Rost *Computational Nuclear Physics* **2** (Eds. Langanke K. *et al.*, Springer-Verlag, 1993) 88.

[18] P. Descouvemont (1995) *Phys. Rev. C* **52** 704–710.

[19] S.C. Pieper, private communication.

[20] S. Ilieva *et al.* (2012) *Nucl. Phys. A* **875** 8–28.

[21] V.V. Burov, V.K. Lukyanov, D.N. Kadrev, and Yu.S. Pol' (1998) *Phys. At. Nucl.* **61** 593.